Modeling analysis for OLED degradation mechanism using impedance spectroscopy

임피던스 분광법을 이용한
OLED 열화 메커니즘에 관한 모델링 분석

BY

HYUNJONG KIM

FEBRUARY 2014

DEPARTMENT OF ELECTRICAL ENGINEERING AND
COMPUTER SCIENCE
COLLEGE OF ENGINEERING
SEOUL NATIONAL UNIVERSITY

M.S. THESIS

Modeling analysis for OLED degradation mechanism using impedance spectroscopy

임피던스 분광법을 이용한
OLED 열화 메커니즘에 관한 모델링 분석

BY

HYUNJONG KIM

FEBRUARY 2014

DEPARTMENT OF ELECTRICAL ENGINEERING AND
COMPUTER SCIENCE
COLLEGE OF ENGINEERING
SEOUL NATIONAL UNIVERSITY

Modeling analysis for OLED degradation mechanism using impedance spectroscopy

임피던스 분광법을 이용한
OLED 열화 메커니즘에 관한 모델링 분석

지도교수 홍 용 택

이 논문을 공학석사 학위논문으로 제출함

2014 년 2 월

서울대학교 대학원

전기컴퓨터 공학부

김 현 종

김현종의 공학석사 학위논문을 인준함

2014 년 2 월

위 원 장 : ＿＿＿＿＿＿＿＿＿＿ (인)

부위원장 : ＿＿＿＿＿＿＿＿＿＿ (인)

위　　원 : ＿＿＿＿＿＿＿＿＿＿ (인)

Abstract

Modeling analysis
for OLED degradation mechanism
using impedance spectroscopy

HYUNJONG KIM

DEPARTMENT OF ELECTRICAL ENGINEERING AND
COMPUTERSCIENCE

COLLEGE OF ENGINEERING

SEOUL NATIONAL UNIVERSITY

Organic light emitting diodes(OLED) was first discovered by W. Helfrich, M. Pole and et al. in 1963 and became gradually known by C.W Tang team at Eastman-Kodak and made green light emitting OLED that had thin film structures. Soon, OLED started to apply to display market as OLED can be fabricated in ultra-thin film structure and operated under low driving voltage. But they have a critical weak point that is chemical compound. Because chemical compound devices are generally weak at moisture, oxidation and heat, the fabrication is carefully progressed to get rid of these and after OLED products are fabricated, encapsulation progress is

absolutely necessary. Other weak point is OLED degradation that appeals after electric power supply. These drawbacks shorten the display life time as well as cause what is called a blur that drops uniformity of display. These drawbacks are fatal fault when OLED competes with other display. Thus effort to slow down the degradation process is gradual issue in OLED study.

This thesis, we noticed that the voltage supply shape can effect to OLED degradation and measured. The result is OLED is more stable when alternated voltage is supplied than when direct voltage is supplied. This result shows that the role of accumulated charge movement in space charge must be noticed in OLED degradation modeling. That is, recombination and luminescence occur in interface of HTL and EML thus the accumulation of charge in this interface cannot avoid causing bottleneck phenomenon and the fixed charge as cation influence OLED degradation. Therefore frequency power supply method can recover the OLEL life time. And as additional study, using impedance spectroscopy OLED modeling is tried. This modeling is added the inductor to notice the negative capacitance that occur in low frequency while the typical OLED model is composed parallel circuit of capacitance and resistance. By this model, each parameter value can be extracted before and after OLED degrades and figure each parameter changes and these result applied to OLED degradation model. As a result, the inductance component is increased and the internal capacitance component is slightly decreased. In addition,

the overall resistance is increased. The increased inductance component can be monitored by the increased value of negative capacitance and this may mean that internal localized electric field that arises by the accumulated charge inside OLED is increase, so that this field impedes injection of the new carrier. In addition, the decreased capacitance means can be analyzed that the effective EML layer thickness is shrink. Thus the degradation phenomenon affects spatial variations of the internal interface. In this study, it revealed that the life time of the OLED is changed by frequency driving method and I developed the mathematical program tool that is able to implement physical meaning and to extract the accurate parameters of equivalent OLED circuit comparatively. As a result, degradation mechanism can be explained by each extracted impedance parameters using impedance spectroscopy. This study is relevant not only to present comparatively simple way that OLED performance can be evaluated but also to support the physical and chemical analysis through OLED electrical analysis in further enlarged, complicated and mass produced OLED industry.

Contents

List of Figures

List of Tables

Chapter 1 Introduction

Introduction

1.1 History

Organic light emitting diodes(OLED) was first discovered by W. Helfrich, M. Pole and et al. in 1963 and became gradually known by C.W Tang team at Eastman-Kodak and made green light emitting OLED that had thin film structures. Soon, OLED started to apply to display market as OLED can be fabricated in ultra-thin film structure and operated under low driving voltage. But they have a critical weak point that is chemical compound. Because chemical compound devices are generally weak at moisture, oxidation and heat, the fabrication is carefully progressed to get rid of these and after OLED products are fabricated, encapsulation progress is absolutely necessary. Other weak point is OLED degradation that appeals after electric power supply. These drawbacks shorten the display life time as well as cause

what is called a blur that drops uniformity of display. These drawbacks are fatal fault when OLED competes with other display. Thus effort to slow down the degradation process is gradual issue in OLED study.

1.2 Issue of OLED life time

There are many studies to make longer the OLED life time. And it can be told that the studies are classified by direct methods and indirect methods. First thing among the direct method to prevent the degradation is to make out the best suited organic compound. It means to find the materials that have resistance to be stable not only oxidation-reduction reactions but also thermodynamic and humidity. But it is very hard to find an epoch-making discovery of chemical compound, so that it required many trials-errors, and much time to study. Second method is inserting additional layers that make carrier's transport characteristic increase, for example hole transport layer(HTL) between anode and emitting layer, electron transport layer(ETL) between cathode and emitting layer, in some cases, hole injection layer(HIL), electron injection layer(EIL) or blocking layer(HBL,EBL) that make carrier concentration increase at emission layer. Due to making OLED band structure more effectively, in these cases, each additional layer makes recombination efficiency of OLED increase so that they help the OLED operated in low voltage

and emit stable luminescence. This method also can reduce influences of the degradation because required electrical stress in active device decrease. And as the indirect method, a compensation circuit in driving circuit is used. The object of this method is usually purport to make consumer not to know the uniformity of display although there is partial of the display degrade in OLED display.

1.3 Frequency dependent of OLED

This thesis, we noticed that the voltage supply shape can effect to OLED degradation and measured. So first, it was performed to measure the change of the OLED IV curve that was varied with frequency voltage driving before and after degradation. The result will be reveal the which OLED under the specific driving environment is more stable. [20]

1.4 Extracted parameter from equivalent modeling

As additional study, using impedance spectroscopy OLED modeling, it is performed to extract the parameters of equivalent circuits. The effective algorithm that can extract each parameter consistently by MATLAB program was developed by author. After the algorithm was applied to the result of the OLED impedance

response, the correlation of the parameter changes with OLED degradation is discussed. Although traditional semiconductor equivalent circuit model usually includes only resistance and capacitance, the modeling in this thesis is added the inductor to notice the negative capacitance that occur in low frequency to approach actual OLED impedance response. [21]

Chapter 2 Theory

Theory

2.1 Impedance spectroscopy

Impedance spectroscopy is an electrochemical technique with broad application that is growing in importance.[1] Impedance spectroscopy is created by Oliver Heaviside by applying Laplace transforms to the transient response of electrical circuit.[2] After that, many scientist developed applications of the impedance spectroscopy to many physical areas, for example measurement of dielectric properties for aqueous electrolytes, galvanic cells semiconductor, electrode and oxides, etc.[3] In 1941, brothers Cole and Cole introduced frequency dependent complex dielectric constant can be represented semicircle in complex impedance domain.[4] In this paper, Cole-cole plot is used as very important tool that can extract each parameter of OLED equivalent circuit component. Equation (2.1) and

(2.2) shows the reason that equivalent circuit compounded by basic component make Cole-cole plot shape become semicircle in complex plan. Figure 2.1 and 2.2 show the Cole-cole plot shape of 4 basic components

$$\frac{1}{A \pm j\omega B} \quad \Rightarrow \quad Z'^2 + Z''^2 = \frac{1}{A}Z' \qquad \omega_{\mathrm{Im}_{max}} = \frac{A}{B} \tag{2.1}$$

$$\frac{1}{A \pm j\dfrac{B}{\omega}} \quad \Rightarrow \quad Z'^2 + Z''^2 = \frac{1}{A}Z' \qquad \omega_{\mathrm{Im}_{max}} = \frac{B}{A} \tag{2.2}$$
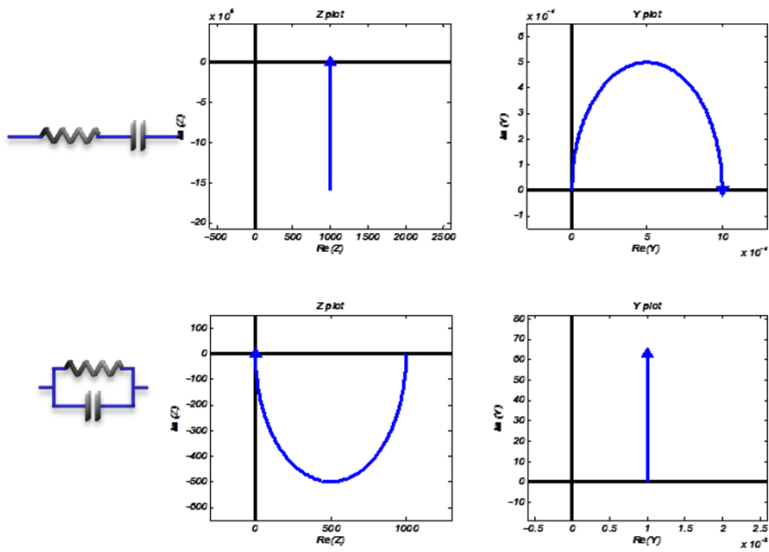
Figure 2.1 Impedance and admittance Cole-cole plot shape of series and parallel circuit compound with resistance and capacitance respectively.
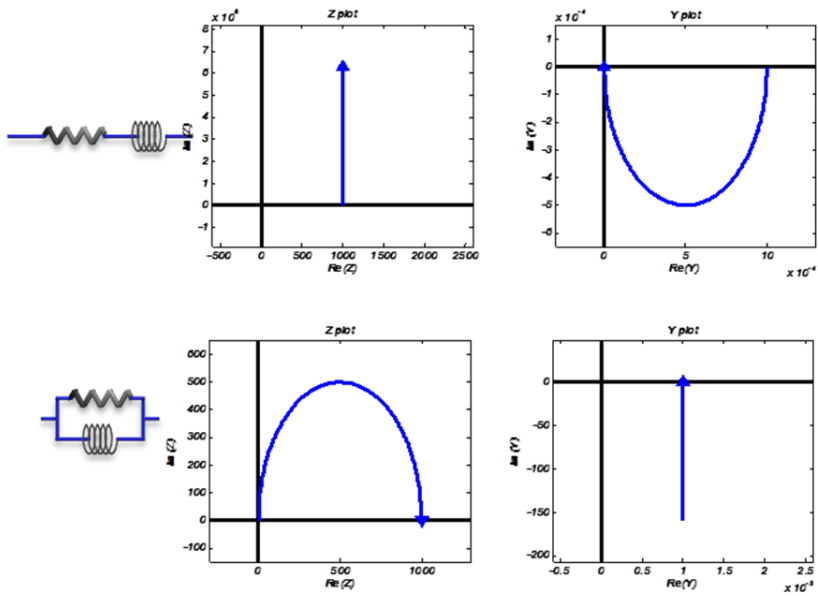
Figure 2.2 Impedance and admittance Cole-cole plot shape of series and parallel circuit compound with resistance and inductance respectively.

As you can see equation (2.1), (2.2) and Figure 2.1, 2.2, resistance of device reflect radius of semicircle and capacitance or inductance can be extracted from resistance and maximum of reactance value

2.2 How to extract reasonable parameter from impedance spectroscopy

Unlike theoretical ideal model, practical impedance response of device is very complicated because the devices usually have various combinations of physics mechanisms. These combinations of physics mechanisms can be depend on chemical reaction of species, mass transfers of carrier, or complicated interface structure. Also though the circuit models are different each other, impedance response can be same. To solve this problem, a consistent strategy is required. After long consideration, I eventually set up the strategy that performed by recursively repeated mathematical programing using MATLAB. This program performs like below orders and flow chart illustrated Figure 2.3. All RCL circuit regard as series of RC or RL parallel circuit that has semicircle because a complicated circuit can be change to which form. Table 2.1 and Table 2.2 show that any complicated circuit fundamentally can be changed to other simple form by the Laplace equation. Therefore if once the simplest circuit model parameters are determined, it is easy to meet any requirement to change circuit model.

1. Draw the Cole-cole plot from the impedance response of the experimental device

2. Extract dominant parameter values(1st) from the largest circle

3. Subtract impedance made by dominant parameter value from largest circle

4. Extract dominant parameter values(2nd) from subtracted data

5. Add first data and Second data

6. Calibrate error between experiment data and extracted data

7. Repeat from 1 step to 6 step

8. If the error is trivial, Subtract impedance made by 1st and 2nd parameter value from experimental device

9. find 3rd extracted values by similar 3, 4 step

10. Repeat all, until total error is trivial
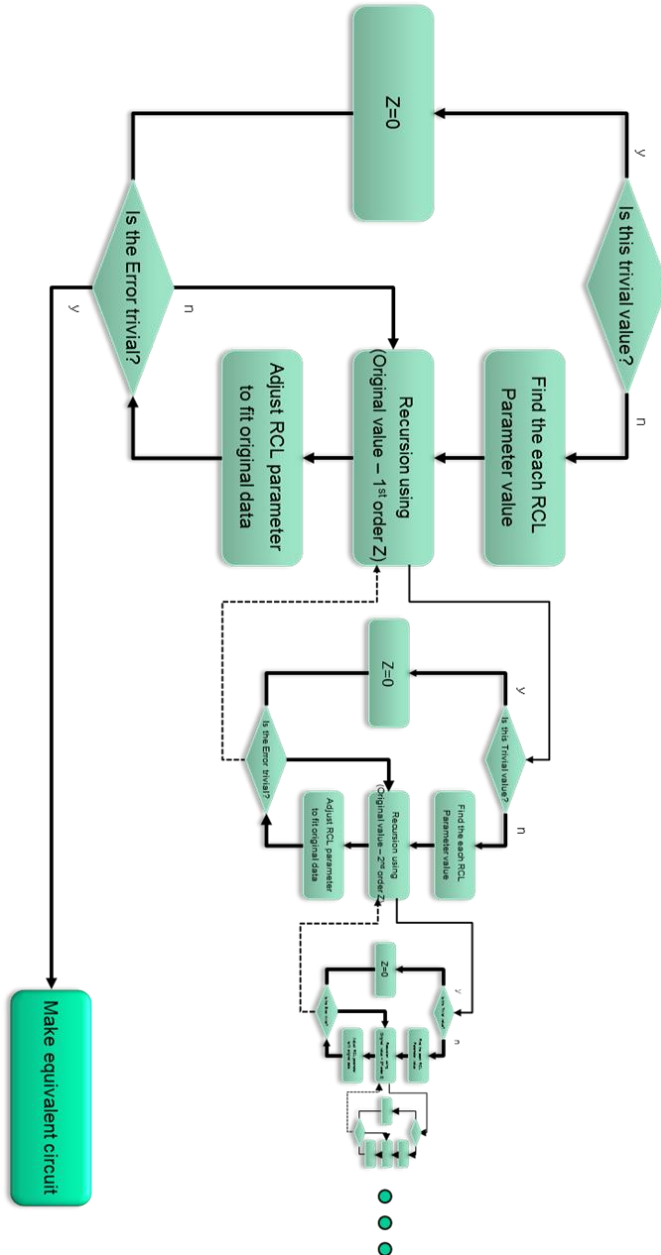
Figure 2.3 Recursion programming flow chart to extract more precise parameter from Cole-cole plot

	$$Z_{1st} = R \parallel \frac{1}{sC} = \cfrac{1}{\cfrac{1}{R} + sC} = \frac{A}{s+\alpha} \qquad ...\left(A = 1/C, \ \alpha = 1/RC\right)$$
	$$Z_{2nd} = R + \frac{1}{sC} = \frac{sRC+1}{sC} = A\frac{s+\alpha}{s} \qquad ...\left(A = R, \ \alpha = 1/RC\right)$$
	$$Z_{3rd} = R \parallel sL = \cfrac{1}{\cfrac{1}{R} + \cfrac{1}{sL}} = \frac{As}{s+\alpha} = A - \frac{A\alpha}{s+\alpha} \qquad ...\left(A = R, \ \alpha = R/L\right)$$
	$$Z_{4th} = R + sL = A(s+\alpha) \qquad ...\left(A = 1/L, \ \alpha = R/L\right)$$
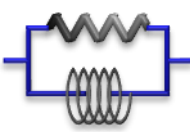
Table 2.1

	$$Z_{5th} = R + Z_{1st} = A' + \frac{A}{s+\alpha} = A\frac{s+\beta}{s+\alpha}$$
	$$Z_{6th} = R \parallel Z_{2nd} = \left(A' + A\frac{s}{s+\alpha} \right)^{-1} = A\frac{s+\beta}{s+\alpha} = A' + \frac{A}{s+\alpha}$$
	$$Z_{7th} = R \parallel Z_{5st} = \left(R^{-1} + A\frac{s+\alpha}{s+\beta} \right)^{-1} = \left(A\frac{s+\alpha}{s+\beta} \right)^{-1}$$ $$= A\frac{s+\beta}{s+\alpha} = A' + \frac{A}{s+\alpha}$$
	$$Z_{8th} = R + Z_{1st} + Z_{1st} = A' + \frac{A}{s+\alpha} + \frac{B}{s+\beta}$$
	$$Z_{9th} = 1/sC \parallel Z_{5st} = \left(sC + A\frac{s+\alpha}{s+\beta} \right)^{-1} = \left(A\frac{s^2+\alpha s+\beta'}{s+\beta} \right)^{-1}$$ $$= A\frac{s+\beta'}{(s+\alpha)(s+\beta)} = \frac{A}{s+\alpha} + \frac{B}{s+\beta}$$
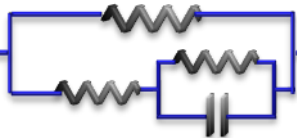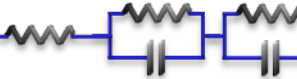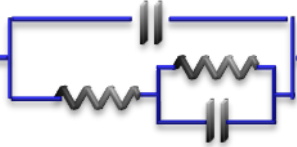
Table 2.2

2.3 Application to the OLED

To verify the developed recursion method, practice impedance measurement data of fabricated OLED is applied to recursion program and the result is illustrated in Figure 2.4. It can be observed that the impedance composed by extracted parameter that successively approach to the practice model curve using debugging mode.
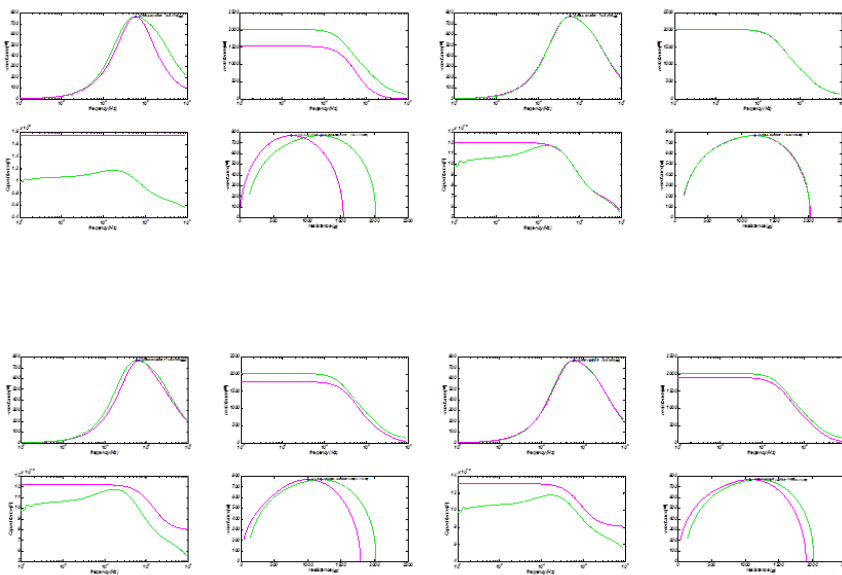
Figure 2.4 Sequential extracting process using developed method. Green lines are the measured original impedance data. Pink lines are approximate lines made by

extracted parameters.

(a)
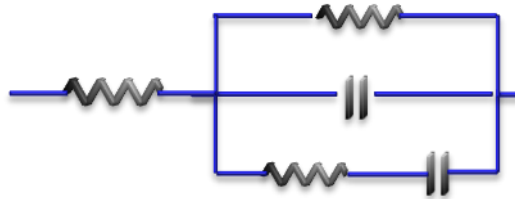
(b)

Figure 2.5 Two mathematically equivalent electrical circuits. (a) is a basic measurement model. (b) is solid-state Schottky diode with leakage current and deep-level electronic states.

Figure 2.4 (a) show the result of the first recursion cycle of the OLED that only demonstrate dominant circle and (b) is second recursion of OLED that demonstrate sub-circle included differential circle. And (c) and (d) is the process of the sequential

adjustment in considering the error and neglecting the trivial values. After that, it is required to extract parameter to reasonable diode model that is able to explain leakage current, trap site and depletion region etc. Figure 2.5 (a) is the rare extracted OLED model from the recursion programing and (b) is the target model that explains the OLED mechanism. So I could extract more reasonable OLED model parameters as converting from (a) to (b).

Chapter 3 Experiments

Experiments

The parallel two experiments were respectively performed at this study. Although each experiment was designed with different purposes at the first, I attempted to compound each result for analysis of degradation of OLED using impedance spectroscopy. The first experiment shows the frequency dependency with OLED degradation. And the second experiment shows the extracted equivalent circuit parameters of the Alq_3 OLED using impedance spectroscopy to try to explain relation of the equivalent circuit response and frequency dependency. So to speak the conclusion, there may be cut off frequency of trap sites or leakage path. Thus the trap sites or leakage paths can be varied by frequency of applied bias and the frequency dependency of the OLED can be explained equivalent circuit response

3.1 Fabrication of OLED for frequency stress

For the experiments of the frequency dependency of the OLED driving voltage shift, we used top-emission blue fluorescent (TBOLED), and bottom-emission blue (BBOLED) and green (BGOLED) fluorescent OLEDs, which were fabricated on glass substrates at Samsung SDI. The ITO substrates were treated with ultraviolet (UV) ozone for 15 minutes and then annealed on a hot plate for 10 minutes. The structure of BBOLED and BGOLED is ITO/HIL/HTL /EML/ETL/LiF/Al. All the OLEDs were encapsulated by glass caps with desiccant. The light emitting area was 4 mm^2.

3.2 Fabrication of OLED for degradation modeling

In this study, we used a bottom emission fluorescent OLED, where we used indium-tin-oxide (ITO) as anode material, 4,4'-bis [N-(1-napthyl)-N-phenyl-amino] biphenyl (α-NPB) as hole transport layer (HTL) material, Alq3 as electron transfer layer/light emissive layer (ETL/LEL) material, and bi-layer of lithium fluoride (LiF) / aluminum (Al) as cathode material, as shown in Fig. 1. Thicknesses of organic and cathode layers were 60, 70, and 0.5/100 nm, respectively. Green light mission was

obtained from the fabricated OLEDs. ITO patterned glass substrates were cleaned according to a conventional cleaning process, treated with ultraviolet (UV) ozone for 15 minutes, and then annealed on a hot plate for 10 minutes. Organic layers and cathode layer were consequently deposited by a thermal evaporation method without breaking vacuum under a high vacuum condition ($2.6\sim4.8\times10^{-6}$ Torr). All the OLEDs were encapsulated by glass caps with desiccant. The light emitting area was 4 mm^2.
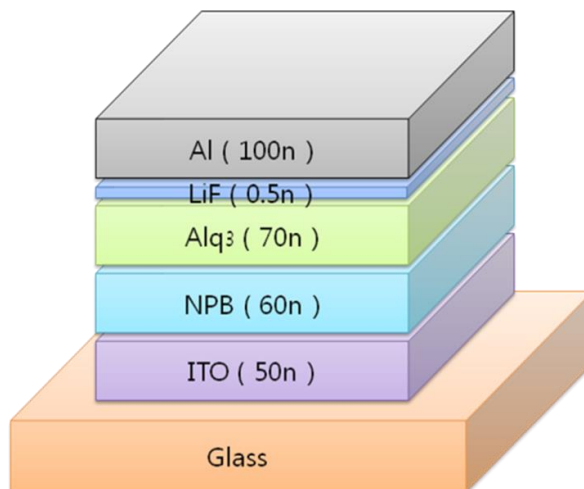
Figure 3.1 Structure of the fabricated OLED
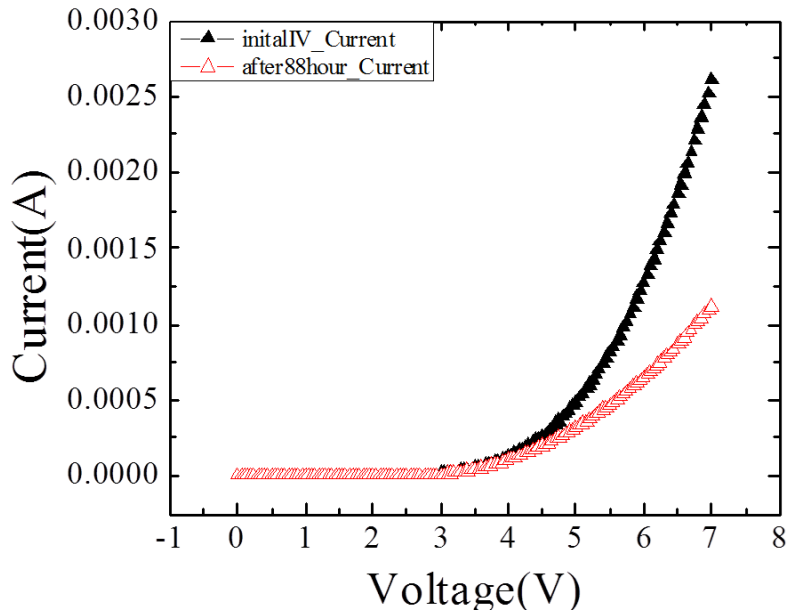
Figure 3.2 characteristics of the fabricated OLEDs before and after the bias stress test for 88 hours

3.3 Measurement for frequency stress

For the OLED performance characterization and bias-stress test, a semiconductor parameter analyzer, HP 4155C, connected with a pulse generator unit, HP 41501B was used. To measure the initial absolute OLED luminance (cd/m^2), we used Minolta luminance meter LS-100. We stressed the OLEDs by applying pulsed voltage signals with 50% duty ratio at several frequencies for a certain period of

time. Then, the stress pulsed voltage signal was intermittently stopped to measure current-voltage (I-V) characteristics of OLED and an OLED voltage at a given constant current level. During I-V characteristics measurement, OLED light output was measured with a photodiode to monitor the luminance change relative to its initial luminance. The photodiode produces photo-current corresponding to the OLED light output or luminance. We carefully optimized the sweep step and range of the sweeping OLED voltage for I-V characteristics measurement so that the contribution of the measurement to the total OLED stress time is minimal. All the device characterization and stress test were performed in the air at room temperature.
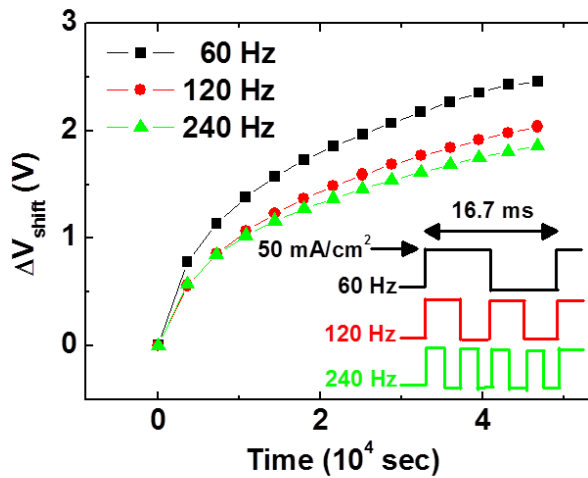
Figure 3.3 TBOLED driving voltage shift and the waveforms used for the stress test

3.4 Measurement for degradation modeling

For OLED current-voltage (I-V) characteristics measurement, we used a semiconductor parameter analyzer, HP 4155C. I-V characteristics were measured and compared as shown in Fig. 2 before and after all bias stress and impedance measurement sequences. OLED impedance was measured by using a LCR meter, HP4284A, which has a bandwidth of 1MHz. The impedance was measured at 7 V DC with 400 mV rms AC oscillation signal every hour during the bias stress test, where a constant voltage (7 V) was applied from HP4284A as the stress bias signal. We used a constant voltage as the bias stress signal because the constant current bias stress was not possible for our Labview-based automatic stress and measurement setup. Total bias stress time was about 88 hours. All the measurements were performed at room temperature in air.

Chapter 4 Results

Results

4.1 Degradation under frequency driving

Table 1 shows the peak voltage (V_{peak}) of the stress pulsed voltage signals and the corresponding peak current density (J_{peak}) and luminance (L_{peak}) at the peak voltage for TBOLED, BBOLED, and BGOLED. Since we used 50% duty ratio in this paper, the averaged luminance (L_{avg}) is the half of the peak luminance, which are 2000, 3000, 5000 cd/m2 for TBOLED, BBOLED, and BGOLED, respectively. We used the relatively high initial luminance conditions to accelerate the degradation process of each OLED. Typical values of the maximum luminance required for 150 cd/m2 maximum luminance of the commercially available hand-held phone are 800-900, 1200-1400, and 700-800 for red, green, and blue OLEDs,

respectively. Although we used the luminance four to five times higher than those required for the commercial applications, our OLEDs showed little change (especially for BBOLED and BGOLED) in luminance and driving voltage after the 60000 sec stress test.

	$V_{peak}(V)$	$J_{peak}(mA/cm^2)$	$L_{peak}(cd/m^2)$	$L_{avg}(cd/m^2)$
TBOLED	7.5~7.8	50	4000	2000
BBOLED	8.2~8.3	75	6000	3000
BGOLED	7.2~7.3	50	10000	5000

Table 4.1 OLED stress conditions

We applied the stress pulsed voltage signals at several frequencies (60~240Hz) to TBOLED to investigate the OLED driving voltage degradation behavior. Figure 1 shows the TBOLED driving voltage shift ($\Delta V_{shift} = V_{stressed} - V_{initial}$) for the initial averaged luminance of about 2000 cd/m^2. $V_{initial}$ and $V_{stressed}$ are voltage values that were measured at a constant current density of 50 mA/cm^2 before and after a certain period of the stress test. In Fig. 1, the schematic description of the stress pulsed voltage signals for 60, 120, and 240 Hz operations are also included. As the frequency of the stress pulsed voltage signals increases, the OLED driving

voltage shift was observed to be suppressed. There was little change in the OLED light-emission efficiency for the stress test performed at several frequencies. The OLED light emission efficiency degraded only a few percent from the initial averaged luminance for all the stress pulsed voltage signals at the several frequencies when the same averaged driving current (thus the same averaged luminance) and the same duty ratio signals were used during the stress test. Table 2 summarizes the values of the TBOLED driving voltage shift during the stress test at 60, 120, and 240 Hz.

Stress time (10^4 sec)	60 Hz	120 Hz	240 Hz
0	7.67	7.76	7.53
2.2	8.42	8.05	7.90
4.3	9.00	8.54	8.34
Total ΔV_{shift}	2.43	1.98	1.81

Table 4.2 TBOLED driving voltage shift during the stress test at several frequencies
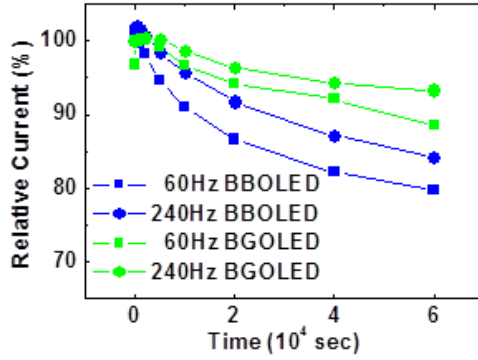
(a)
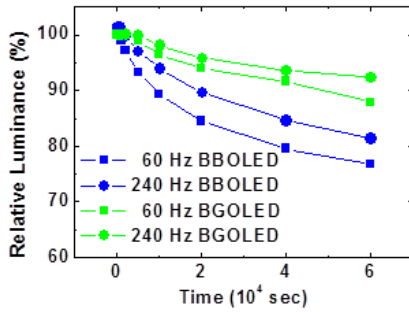
(b)
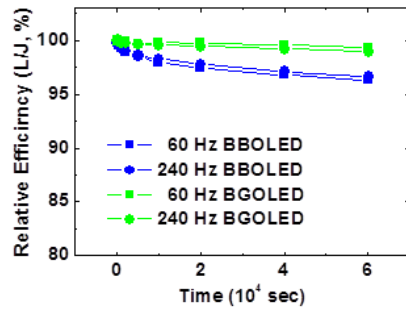
(c)

Figure 4.1 Change of (a) current, (b) luminance, and (c) calculated efficiency for BBOLED and BGOLED. Current and luminance were measured at a constant voltage that is the peak voltage value of the stress pulsed voltage signals for each device

	BBOLED		BGOLED	
	60 Hz	240 Hz	60 Hz	240 Hz
Current	79 %	84 %	88 %	93 %
Luminance	76 %	81 %	88 %	92 %
Efficiency	96.3 %	96.7 %	99 %	99.3 %

Table 4.3 Change of (a) current, (b) luminance, and (c) calculated efficiency for BBOLED and BGOLED. Current and luminance were measured at a constant voltage that is the peak voltage value of the stress pulsed voltage signals for each device.

To further analyze the dependency of OLED driving voltage on the driving frequency, we used the same method for BBOLED and BGOLED. We monitored both OLED current and luminance changes at a given OLED driving voltage during the pulsed voltage stress test at frequencies of 60 and 240Hz. Figure 2 shows the change of the current flow, luminance, and calculated efficiency of OLEDs from their initial values for BBOLED and BGOLED. For the calculated efficiency, the measured luminance was divided by the measured current. All the relative values show the percent ratio of the stressed value to the initial value.

The current and luminance were measured at constant voltages of 8 and 7.2 volts for BBOLED and BGOLED, respectively. These voltage values are the same as the peak voltage that were used for the pulsed voltage stress as shown in the Table 1. It is shown in Fig. 2 that the reduction of current and luminance (thus, degradation of OLED performance) were suppressed when the 240 Hz pulsed voltage signal was used for the stress test in comparison with the result of the 60 Hz pulsed voltage signals. After 60000 sec stress time, the current flow through the BBOLED and BGOLED for the same driving voltage was reduced to 79 and 84% of the initial current flow for the pulsed voltage stress test at 60 Hz. Since OLED luminance is typically proportional to the current flow through the OLED, the luminance change follows the tendency of the current flow change. However, the absolute amount of the luminance degradation can be different from that of the current flow degradation when the OLED efficiency cd/A degradation is differently affected by the stress pulsed voltage signals with 60 and 240 Hz frequencies. From Fig. 2(c), the efficiency degradation is little affected by the frequency of the OLED driving voltage. Difference in the amount of the efficiency reduction for 60 and 240 Hz is only less than 0.4% for both devices after 60000 sec stress time. The change of current flow, luminance, and calculated efficiency is summarized in Table 3. If we define the lifetime of OLED (95% lifetime) at the time when the luminance drops to 95% of the initial luminance, the lifetime of BBOLED and BGOLED is 3600 and

15700 second, respectively, for the 60 Hz stress conditions. The lifetime has been increased to 8300 and 27300 seconds for BBOLED and BGOLED, respectively, for the 240 Hz stress conditions. If we compare the driving voltage shift at the end of the about 40000 sec stress time of TBOLED and BBOLD, the BBOLED showed the better device stability with less than 5% increase (V_{shift}/V_{peak} = 0.4/8.2~8.3) from the initial driving voltage value while the TBOLED showed about 25% (V_{shift}/V_{peak} = 2.43/7.5~7.8) increase. It is noted that the more accelerated initial stress conditions were used for BBOLED (Table 1). Therefore, for blue OLEDs, bottom-emission type OLED showed the much better device stability in comparison with the top-emission counterpart.[20]

4.2 Each extracted parameter of Alq$_3$ OLED degradation

Figure 4.1 shows Cole-Cole plots of the measured OLED impedance and their changes with the stress time. Horizontal and vertical axes represent resistance and reactance, respectively. Positive reactance was observed at low frequency for both fresh and aged devices. This positive reactance is directly related to the NC of OLEDs, which was previously reported by other groups. Over the frequency ranges where the OLED has positive reactance, resistance component increases from about

500 ohm until the OLED reactance becomes negative. As the frequency further increases, the OLED resistance decreases while the reactance increases in its magnitude from zero up to certain frequency range and then decreases toward zero. We used the frequency range from 20 Hz to 1 MHz, which is a typical frequency range available from HP4284A. As the stress time increases, the contour of the Cole-Cole plots spreads outwardly as indicated with black arrows in the figure. If we have a good circuit model representing this Cole-Cole plot results, we can extract parameter values of each element in the model by using a conventional mathematical program tool. Although there have been many attempts to accurately model the Alq3-based standard OLEDs[4][5][6], Pingree's equivalent circuit model best represents the NC behavior of the OLEDs, where Alq3 layer was modeled as a parallel connection of a resistor (R_C) and a capacitor (C), α-NPB bulk layer was modeled as a parallel connection of a resistor (RL1) and an inductor (L1), and the interface between α-NPB and ITO anode as a series connection of a resistor (R_{L2}) and an inductor (L_2), as shown in Fig. 4.3[3][7].
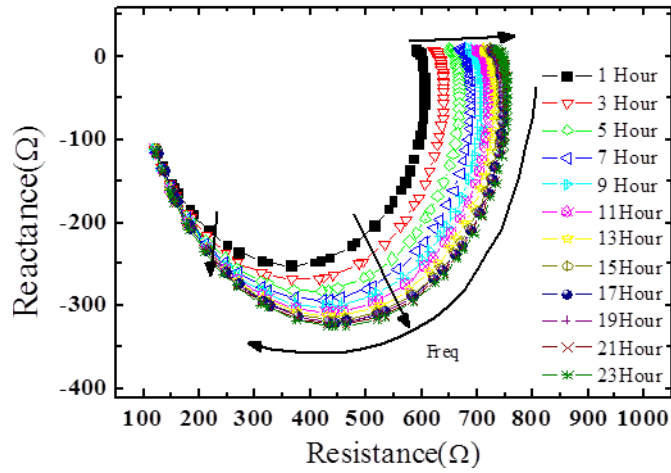
Figure 4.2 Cole-Cole plots of the measured OLED impedance and their changes with the stress time

ITO is represented as a resistor (RS) Total impedance of the OLED equivalent circuit model can be represented as the following equation.

$$Z_{total} = R_s + (R_c \,||\, 1/j\omega C) + ((R_{L1} \,||\, j\omega L_1) \,||\, (R_{L2} + j\omega L_2)) \qquad \textbf{(4. 1)}$$
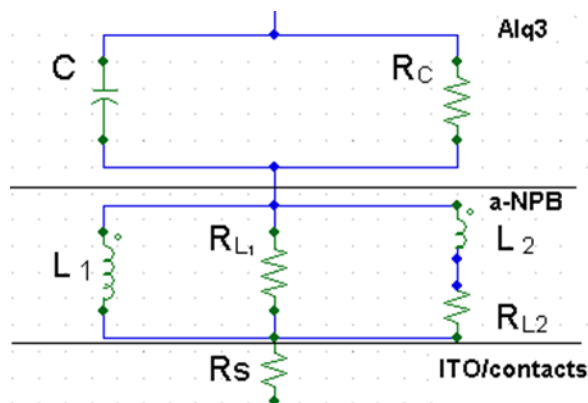
Figure 4.3 OLED equivalent circuit model used in this study

By comparing impedance behaviors of both equation (4.1) and measured data, we were able to successfully extract each element value. Figure 5 shows changes in each extracted element value with the stress time. While all the resistance and inductance increased with the stress time, capacitance decreases with the stress time. Although it is very difficult to accurately relate each parameter change with the degradation behavior and pose any physical meaning on the change, some of the parameter change can be explained as follows. Change of RC can be considered as change in the bulk transport properties of the Alq3 layer. RL1, RL2 can be also explained in a similar manner. As the organic material and layer degrades, defect or trap sites can increase in the bulk layers, impeding charge carrier movement and thus, resulting in changes in resistance of the bulk layers. As mentioned before, since the NC is related to various physical phenomenons, we do not have a clear explanation for the changes in L1 and L2, which are under current intense investigation. However, both inductance values increase with the stress time and it is speculated that this phenomenon is related to the charge accumulation at the organic interface and corresponding electric field redistribution in the OLED as the device degrades.

Regarding change in capacitance value with the stress time, the extracted value decreased from 1.49 nF to 1.44 nF after the OLED degraded. Capacitance is closely related to dielectric constant, area, and thickness of the Alq3 layer. It is

assumed that there is negligible change in dielectric constant and area during the stress time period that we are considering. In fact, when we observed the aged device under the microscope, we did not observed reduction in the light-emitting area of our OLEDs. The thickness or effective distance for electron transport from cathode to the recombination zone possibly changed as the device degraded. Degradation induced recombination zone shift or change of the light-emitting zone depth change with degradation have been already reported for mixed host and conventional Alq/diamine (TPD) based OLEDs, respectively. In the mixed host OLED, it was reported that the recombination zone was formed in the light-emitting layer 10 nm away from the interface of light-emitting layer and hole transport layer, and then the recombination zone shifted to the interface and became broaden as the device degraded. For the conventional Alq based OLEDs, it was reported that the recombination zone was distributed in the Alq layer up to about 20 nm away from the Alq/TPD interface and shrank toward the interface as the device degraded. Although we do not have experimental results for this type of recombination zone variation with the stress time at this stage, we believe that in our device, there should be also similar shift or shrinkage of the recombination zone as the device degrades, which can effectively change the distance for electron transport from cathode to the recombination zone, resulting in increase and decrease of RC and C, respectively.[21]
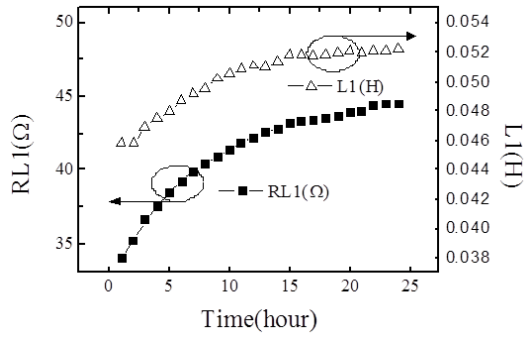
(a)
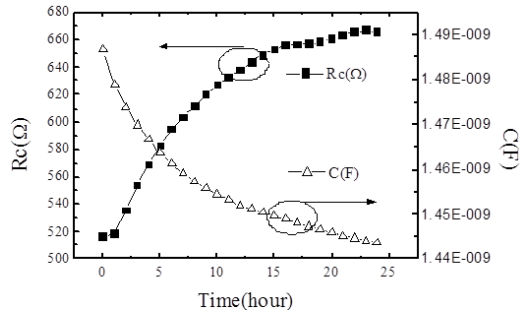
(b)
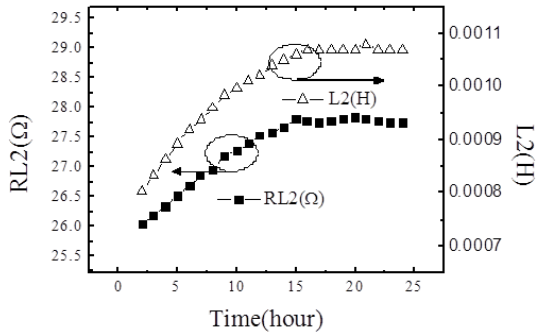
(c)

Figure 4.4 Changes in extracted parameter values with the stress time for (a) resistor and capacitor modeled for Alq3 layer, resistor and inductor modeled for (b) α-NPB bulk & (c) interface of α-NPB/Alq3. All the parameters were extracted from Cole-Cole plot of the measured data and equation (1).

Chapter 5 Discussion

Discussion

5.1 Effects of frequency driving

In this study we can find out that the OLED degradation is related to driving frequency. Based on our result, 240 Hz operation of OLED showed smaller OLED driving voltage shift in comparison with 60 Hz operation for TBOLED, BBOLED and BGOLED, after the same amount of the pulsed voltage stress time. Thus, the 95% lifetime of BBOLED and BGOLED has been increased by almost two times when 240 Hz stress conditions were used. We are currently further investigating this frequency dependence of OLED driving voltage shift at other frequencies for several

OLED devices. Based on our preliminary result, it may not be expected that the suppression effect monotonously increases as the operation frequency increases. There can be an optimal frequency to produce the best suppression effect for each type of OLED. By combining the optimization of the operation frequency and the duty ratio driving method, further improvement of OLED lifetime is expected; thus, the improved lifetime of digitally driven AMOLED can be obtained. Simple digital driving method will give a big benefit to AMOLED technology, such as further reduction of fabrication and driving cost of AMOLED.

5.2 Consideration of the Negative capacitance as carrier impeding effect

In the past decades, the negative capacitance have been known for unusual capacitance behavior, but observed in a variety of semiconductor devices. For decades, although many studies tried to brighten up the negative capacitance behavior, there is only partial understanding of the negative capacitance behavior.[11]-[18] Among them, the negative capacitance is closely related to non-equilibrium transient electron injection[16] and recombination behavior [17][18].
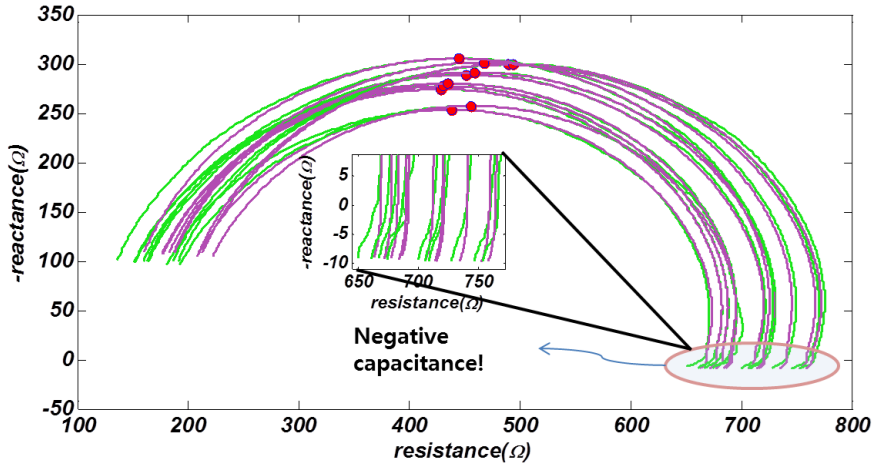
(a)
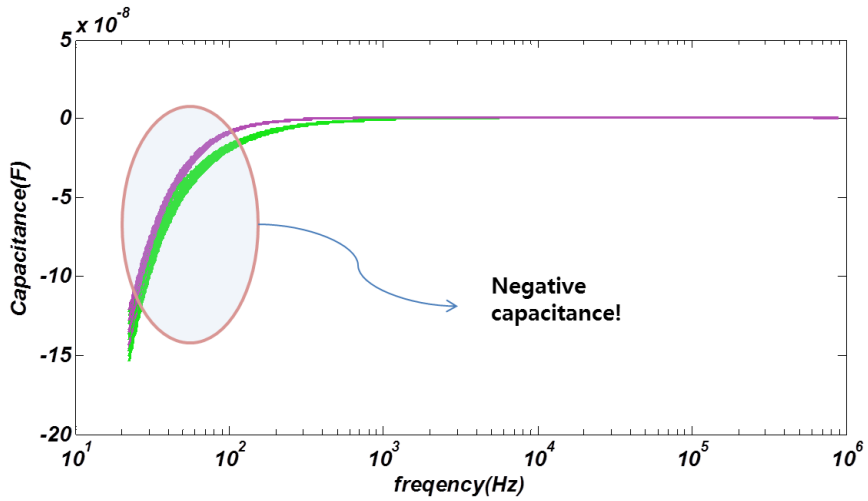
(b)

Figure 5.1 (a) Negative capacitance in Cole-cole plot as Alq3 OLED degradation. The inset shows enlarge of the negative capacitance of impedance response of the OLED. (b) Capacitance-frequency plot shows negative capacitance appeal at low

frequency. Grin lines are practical experiment data, while purple lines are reproduced data extracted by equivalent circuit.

As you can see in this study, the negative capacitance is observed at low frequency. Figure 5.1(a) shows the Cole-cole plot of the Alq3 OLED that used in section 3.2 and Figure 5.1(b) shows the capacitance response of frequency domain. Figure 5.1 apparently show the existence of the negative capacitance in Alq3 OLED impedance response.

5.3 Suggestion another model that can explain the recombination arms and negative capacitance

In section 4, I already extracted the parameter of OLED before and after degradation using Pingree's model.[9] Pingree's model explains the negative capacitance behavior as parallel combination of inductance-resistance of a HTL and accumulation charge, space charge, trap site in EML as parallel combination of capacitance-resistance. It can be reasonable when the bias is distributed at HTL and EML evenly. But at high potential, there is most of the potential is at EML, HTL's role is dwindle away. So I cannot avoid finding other model.

As a result of further study, I referred to the equivalent circuit in a paper written by T. Okachi group. The equivalent circuit includes the junction capacitance, resistance as leakage current path, bulk or electrode resistance and each trap site path. The interesting thing in this equivalent circuit is that additional series of the resistance-inductor is created as a recombination path and negative capacitance contribution.   Figure 5.2 show the equivalent circuit below EL threshold (a), and above EL threshold (b).

(a)   (b)
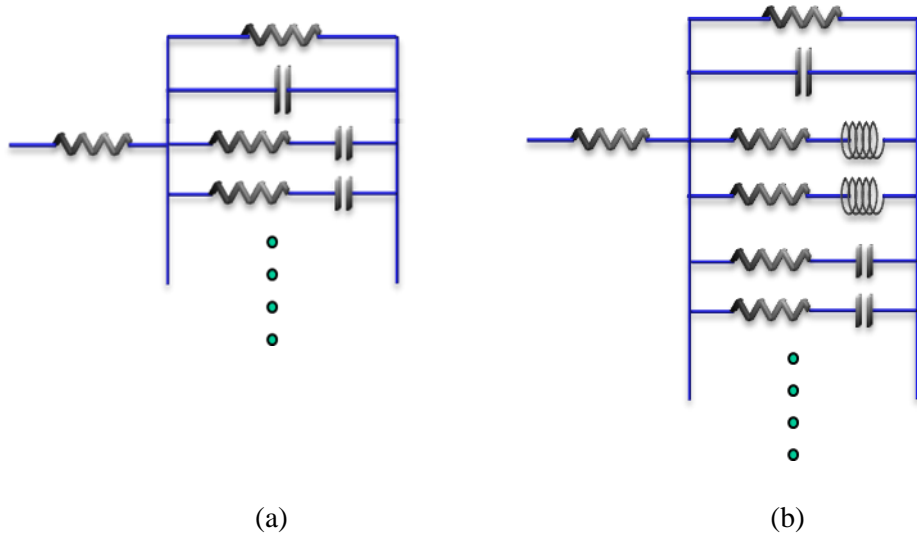
Figure 5.2 Equivalent circuit modeling suggested by H. Azuma et al[19]. (a) equivalent circuit of OLEDs below EL threshold, (b) equivalent circuit of OLEDs above EL threshold.

5.4 Possibility of determining a recombination path by frequency-selective

I used impedance spectroscopy method to investigate OLED degradation behavior by using suggested element circuit model in this section and extracting each parameter values. Figure 5.3 show the changes of the each parameter value, R_C, C, R_{L1}, L_1, R_{L2}, L_2 respectively. All of the resistance and capacitance increase while the inductances decrease. The result is very similar to Pingree's model referred in section 4.
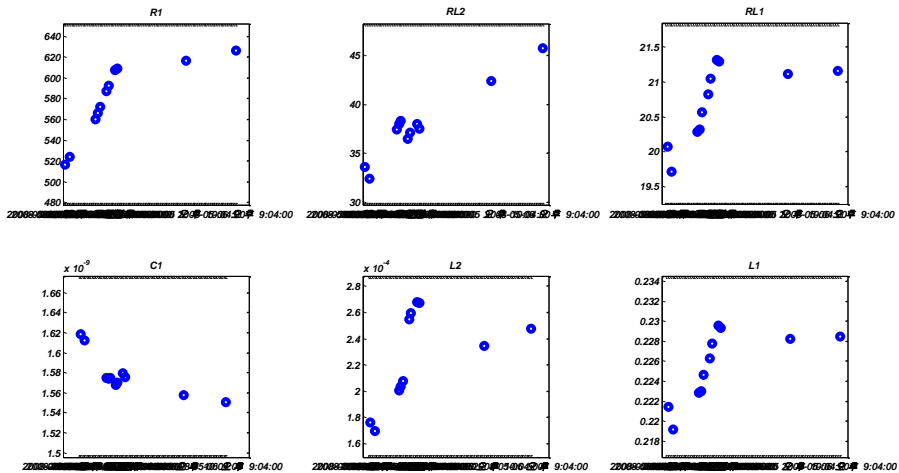
Figure 5.3 Converted parameters from new model in this section respectively (a) R_{C1} (b) R_{L2} (c) R_{L1} (d) C_1 (e) L_2 (f) L_1

Figure 5.4 show how close the practical data and simulation data from extracted parameter.   In this section, I suggest the possibility of determining the recombination path by frequency-selective. As you can see the equivalent circuit model, the path of recombination or carrier hoping trap can be controlled by frequency driving. According to the paper, negative capacitance behavior is as "frozen" factor by recharging processes at the trap site so that the device has carrier impeding effect against new injection carrier. If we can select the driving frequency unfreezing the state operated by main recombination zone that emit target luminescence, and freezing the state operated by trivial recombination zone that cannot luminescence, it is good method carrier control approached by frequency driving.
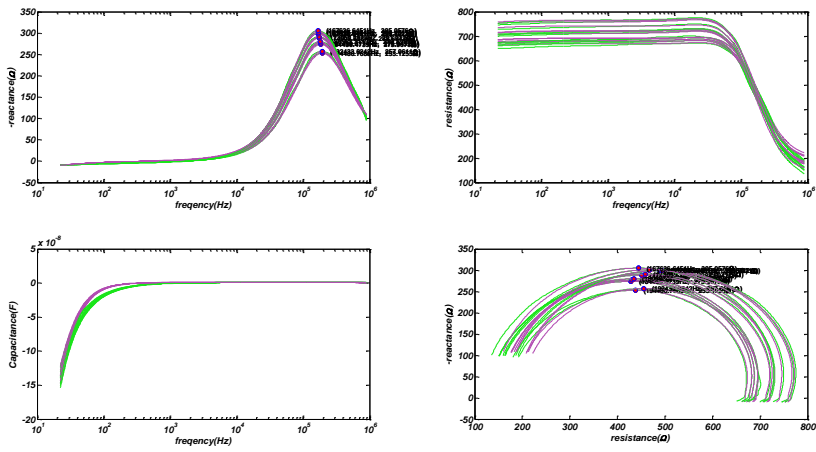
Figure 5.4 Green curves are measured practical OLED impedance data and purple curves are composed with each extracted and adjusted parameter. The horizontal axis is log scale frequency and vertical axis is (a) reactance (b) resistance (c) capacitance respectively. And (d) is Cole-cole plot.

Chapter 6 Conclusion

Conclusion

So far, we examined the impedance spectroscopy of OLED in accordance with degradation and analyzed the mechanism of it. As mentioned in the text, the parameter of OLED, at the first, is extracted from simplified circuit model and, at the second, applied to complex model using mathematical tool.(MATLAB programming) This sequential process is useful to evaluate to properties and defect of semiconductor because the impedance response of device is very complicate. From this method, we effectively extracted each the capacitance values and resistances the before and after of OLED which is stressed by constant voltage. We observed resistance increased and capacitance decreased. This phenomenon can be explained that the carriers which can play a major role of recombination at the homo or lumo level may be swept in the form of leakage current thorough unwanted path

way. Unwanted path way can be created by additional surface stats lowering barrier of the interface or additional deep state in accordance with degradation. So that, increase of resistance represents longer path way and decrease of capacitance represents disappearance of the carrier which could wait for recombination time. Also we observed the negative capacitance in OLED device modeling. This negative capacitance is modeled as inductance and success to extract parameter using mathematical tools. This phenomenon can be represented as freezing role of any states in the semiconductor. As you can see in this paper, OLED characteristic can be influenced, first, device performance and, second, life time. So that if proper the frequency is selected, specific stats may be controlled to freezing the path of the trap. In this paper, the OLED under specific frequency bias has more life time than that of DC bias. Of course, consideration of freezing frequency is useless under DC driving device. Current trend of display industrial, however, demands the high frequency driving controller more and more because of the application of desire of high definition quality and advent of 3D display. Thus it is helpful to find proper frequency bias that cut off specific trap path. Although a delicate quantitative analysis was not performed in this paper, if more reasonable modeling parameters extracted using impedance spectroscopy method performed this study can be obtained, pre-strategies of fabrication of suitable device structures and selection of material and fabrication process is possible in the future.

Bibliography

[1] Mark E. Orazem, Bernard Tribollet "ELECTROCHEMICAL

IMPEDANCE SPECTROSCOPY", A JOHN WILEY & SONS, INC.,

PUBLICATION, 2008

[2] O. Heaviside, Electrical papers, VOLUME 1, New York: MacMillan,

1894

[3] C. H. Ayres, "Measurement of the Internal Resistance of Galvanic

Cell", Physical Review(Series 1), 14, 1902

[4] K. S. Cole and R. H. Cole, "Dispersion and Absorption in

Dielectrics 1: Alternating Current Characterisitic", Journal of

Chemical Physics, 9, 1941 341-351

[5] L.S.C. Pingree et al, "Negative capacitance in organic light-emitting diodes", Appl. Phys. Lett. 86, 073509 (2005)

[6] S.H. Kim et al, "Impedance spectroscopy of single- and double-layer polymer light-emitting diode", J. Appl. Phys. 87, 882 (2000)

[7] Ángeles Pitarch et al, "Impedance of space-charge-limited currents in organic light-emitting diodes with double injection and strong recombination", J. Appl. Phys. 100, 084502 (2006)

[8] S. M. Han et al, Mol. Cryst. Liq. Cryst., Vol. 470 (2007)

[9] L. S. C Pingree et al, "Field dependent negative capacitance in small-molecule organic light-emitting diodes", J, Appl. Phys. 100, 044502 (2006)

[10]   C.-A. Tseng et al, Proc. CLEO/Pacific Rim, 1, (2007)

[11]   M. Matsumura et al, "Change of the depth profile of a light-

emitting zone in organic EL devices with their degradation", Synth.

Met. 91, 197 (1997)

[12]   H. H. P. Gommans, et al, "Negative capacitance in low-

mobility solids", Phys Rev B, 72, 235204 (2005)

[13]   Mieko Matsumura and Yutaka Hirose, "Negative capacitance

Effect in Forword-Biased Metal Oxide Semiconductor Tunnel

Diodes(MOSTD)", Jpn. J. Appl Phys, Vol. 39 (2000)

[14]　A. G. U. Perera et al, "Negative capacitance of GaAs homojunction far-infrared detector", Appl. Phys. Lett. 74, (1999)

[15]　Juan Bisquert et al, "Negative capacitance caused by electron injection through interfacial states in organic light-emitting diodes", Chem. Phys. Lett. 422 (2006)

[16]　Takayuki Okachi et al, "Equivalent circuits of polymer light-emitting diodes with hole-injection layer studied by impedance spectroscopy", Thin Solid Films. 517, (2008)

[17]　M. Ershov et al, "Unusual capacitance behavior of quantum well infrared photodetectors", Appl. Phys. Lett. 70, 14 (1997)

[18] M. Ershov et all, "Negative Capacitance Effect in Semiconductor Devices", IEEE Transactions on electron devices, 45, 10 (1998)

[19] H. Azuma, et al. "13th int. Display workshopws in conjunction with Asia Display, Takamatsu, Japan, 6-9 p 757 (2005)

[20] H. Kim, J. Yang, S. Ye, C. Lee, and Y.Hong∗, "OLED degradation mechanism study using impedance spectroscopy," IMID/IDMC/Asia Display, Oct. 13-17, 2008.

[21] H. Kim, S. Kim, S.W. Chang, D. Lee, D.S. Jeong, H.K. Chung, and Y.Hong ∗, "Frequency dependence of OLED voltage shift degradation," IMID '07, Aug. 2007

Publications

Journal Papers (SCI)

[1] H. Kim, S. Kim, and Y. Hong*, "Frequency Dependency of Multi-layer OLED Current Density-voltage Shift and Its Application to Digitally-driven AMOLED", Journal of the Optical Society of Korea, 16, 181 (2012) (SCI-E)

Conference

International

[1] H. Kim, J. Yang, S. Ye, C. Lee, and Y.Hong*, "OLED degradation mechanism study using impedance spectroscopy," IMID/IDMC/Asia Display, Oct. 13-17, 2008. (oral)

[2] H. Kim, S. Kim, S.W. Chang, D. Lee, D.S. Jeong, H.K. Chung, and Y.Hong *, "Frequency dependence of OLED voltage shift degradation," IMID '07, Aug. 2007 (oral)

[3] H. Kim and Y.Hong *, "Degradation Behavior of OLED under Analog and Digital Driving Conditions," The 4th International Workshop on Nanoscale Semiconductor Devices, Apr. 5-6, 2007. (poster)

Domestic

[1] 홍용택 *, 김현종, 양지훈, 전기적 분석법을 이용한 유기 발광 다이오드의 특성 연구," 광전자 및 광통신 학술대회, May 13-15, 2009 (초청논문)

[2] 김현종, 노승욱, 이창희, 홍용택, "주파수에 따른 임피던스 변화를 이용한 OLED 소자의 열화 분석," 대한전자공학회 추계 학술대회, Nov. 24 2007

국문 초록

Organic light emitting diodes(이하 OLED)는 1963년 W.Helfrich, M. Pope 등에 의해 처음 발견된 이 후, 1987년 Eastman-Kodak 사의 C.W Tang 팀에서 얇은 박막구조의 녹색 발광 소자를 만들어 냄으로 점차 대중에 알려지기 시작 하였다. OLED는 얇은 박막구조로 만들 수 있는 데다 상당히 낮은 구동 전압을 가지고 있는 장점으로 display 산업의 상업적 개발에 곧 적용되기 시작하였다. 하지만 OLED의 최대 결점은 곧 유기화합물이라는 근본적인 태생에 있었다. 유기 화합물은 대개 수분과 산화와 열에 대해 상당이 낮은 안정성을 가지고 있기 때문에 제작 시 이러한 외부요인을 최대한 제거 시켜야 하고, 완제품을 만든 후에도 고도의 봉지작업이 필수적으로 필요하다. 또 다른 단점으로는 전압 공급 시 나타나는 OLED 열화 현상이다. 구동 시 OLED의 발광특성이 나빠진다는 사실은 display의 자체의 수명을 단축시킬 뿐만 아니라, 부분적 열화로 화면의 질이 고르지 못하게 되는 이른바 blur 현상의 주된 원인이 된다. 이는 타 제품과의 경쟁력을 떨어뜨리는 OLED의 가장 치명적인 단점이 된다. 따라서 구동 시 열화를 막으려는 시도는 OLED 연구에서 꾸준히 이어지고 있는 이슈이다.

본 연구에서는 OLED의 전압공급의 방법에 따라 OLED의 수명에 미

치는 영향을 주목하여, 이를 측정하였다. 실험 결과 OLED는 전압이 직류에서 보다 고주파의 구형파의 형태로 공급될 때 보다 좋은 안정성을 보였다. 이는 OLED의 열화 모델에 있어서 공간전하 중 축적된 charge의 역할을 보다 주목해야 한다는 것을 보여 준다. 즉, 보통 HTL과 EML 사이의 계면에서 주로 recombination 과 이에 따른 발광이 나타나는데 이 부분에서의 전하 축적 현상은 항상 병목현상을 나타낼 수밖에 없고 이 중 캐타이온(cation)과 같은 고착된 전하가 열화에 영향을 미친다는 것을 설명 할 수 있다. 이는 OLED 내부로 홀의 주입에 있어서 OLED 인터페이스 내부에 고착된 전하의 상태가 전압 공급의 방법에 따라서 회복 될 수 있다는 것을 의미한다. 이에 따른 추가적 연구로 Impedance spectroscopy를 이용하여 OLED 모델링을 하였다. 이 모델링은 과거의 저항과 캐패시턴스의 병렬연결의 고적적인 모델에서 탈피하여 저주파에서 주로 나타나는 OLED의 Negative capacitance 값에 주목을 하여 인덕터를 추가하였다. 이에 따라 각 파라미터 값을 추출해 내었으며 열화 전후에 따라서 내부의 파라미터가 변화하는 과정을 도식 하였고 이를 열화 모델에 적용 시켰다. 그 결과 내부의 인덕턴스 성분은 증가 하였으며, 캐패시턴스 성분은 약간 감소하였다. 또한 전반적인 저항 값은 증가하였다. 이는 내부의 인덕턴스 성분이 늘어났다는 것은 내부적으로 Negative capacitance의 값이 증가하였다는 것을 의미하고 이는 곧 축적된 전

하가 OLED 내부 전계에 주는 impeding 현상으로 인해 새로운 정공의 주입을 막게 되는 현상이 늘어났음을 의미한다. 또한 캐패시턴스가 줄었다는 사실에서 Alq3의 유효 거리가 줄어든 것으로 해석 될 수 있다. 따라서 열화는 내부 인터페이스의 공간적인 변동에 영향을 준다고 생각 할 수 있다.

 본 연구를 통해서 OLED는 주파수 구동 시 신호의 주파수에 따라 수명이 변화한다는 것을 밝혔으며, 이에 더하여 주파수에 따라 OLED의 임피던스를 측정하여서 등가회로 모델의 파라미터들을 추출 하여 열화 매커니즘을 밝혔다. 이는 향후 점점 대형화 되고 대량 생산화 되고 있는 OLED 산업에 있어서 비교적 간단한 방법으로 OLED 성능을 평가할 수 있는 방법을 제시할 뿐 아니라, OLED의 열화를 전기적으로 해석함으로서 말미암아 이를 다시 근본적인 OLED의 물리적 화학적 분석을 뒷받침 해줄 수 있는 연구로서 큰 의의가 있다.